

Real-Time Digital Signal Processing of Ionization Current for Engine Diagnostic and Control

Gerard W. Malaczynski and Michael E. Baker
Delphi Corporation, Technical Center Brighton

**Reprinted From: Combustion and Flow Diagnostics
(SP-1748)**

All rights reserved. No part of this publication may be reproduced, stored in a retrieval system, or transmitted, in any form or by any means, electronic, mechanical, photocopying, recording, or otherwise, without the prior written permission of SAE.

For permission and licensing requests contact:

SAE Permissions
400 Commonwealth Drive
Warrendale, PA 15096-0001-USA
Email: permissions@sae.org
Fax: 724-772-4028
Tel: 724-772-4891



For multiple print copies contact:

SAE Customer Service
Tel: 877-606-7323 (inside USA and Canada)
Tel: 724-776-4970 (outside USA)
Fax: 724-776-1615
Email: CustomerService@sae.org

ISSN 0148-7191
Copyright © 2003 SAE International

Positions and opinions advanced in this paper are those of the author(s) and not necessarily those of SAE. The author is solely responsible for the content of the paper. A process is available by which discussions will be printed with the paper if it is published in SAE Transactions.

Persons wishing to submit papers to be considered for presentation or publication by SAE should send the manuscript or a 300 word abstract of a proposed manuscript to: Secretary, Engineering Meetings Board, SAE.

Printed in USA

Real-Time Digital Signal Processing of Ionization Current for Engine Diagnostic and Control

Gerard W. Malaczynski and Michael E. Baker
Delphi Corporation, Technical Center Brighton

Copyright © 2003 SAE International

ABSTRACT

Combustion quality diagnostic techniques utilizing flame ionization measurement, with the spark plug as a sensor, have been in production for some time. This acquired "ionsense" signal represents the changes in the electrical conductivity of the flame during each combustion event. The present analog versions of this sensor are used to detect knock and engine misfire, and can be used for cam phasing. However, current methodology has fallen short of unlocking the wealth of combustion thermodynamics information encrypted in the ion sense signal.

Digital Signal Processing incorporating Artificial Neural Networks (ANN) is well suited for handling the statistical fluctuations of combustion. However to obtain acceptable accuracy, traditional ANN implementations can require processing resources beyond the capability of current engine controllers. Using Air/Fuel Ratio and Location of Peak Pressure as examples, this paper explores the practicality of performing real-time digital processing of the ionsense signal to extract additional combustion information. An assessment of required processor resources is made and alternative pre-processing employing a pattern recognition wavelet filter is proposed. As a result the post-processed signal seems to be immune to some engine combustion fluctuations not included in the ANN training.

The concepts discussed were successfully demonstrated throughout the normal operating range, in real-time, on a 6-cylinder engine. Examples of performance data are included.

INTRODUCTION

Theoretical foundations linking the ionsense signal with engine thermodynamics and combustion kinetics were laid by a group of scientists at Lund Institute of Technology, Sweden [1, 2]. The attempt, however, fell short of producing a robust theoretical model since the modeling of molecule formation and destruction kinetics in combustion, even if simplified, is extremely complex (see e.g. [3]). Consequently, the numerous attempts to demonstrate ionsense "advanced functionality", i.e. the ability to provide information on the location of peak pressure, air to fuel ratio, percentage of mass fraction burned, etc., proved to be successful only in a narrow range of automotive engine operating conditions [1 – 7] (leading papers are quoted here only).

As was pointed out in numerous publications, fuel type, fuel additives [8], and fluctuation in early flame development [9] made the interpretation of the ionsense signal extremely difficult. Remembering that air humidity, spark plug performance, engine aging, etc. may also affect the combustion process; a straightforward interpretation of the ionsense signal appears to be almost impossible. Consequently, conventional analytical methods surely do not provide the robustness expected for mass production applications. In an attempt to solve this formidable problem, Halmstad University scientists together with Mecel, an independent subsidiary of Delphi Corporation, proposed the application of artificial neural networks (ANN) for ionsense data interpretation (see e.g.: [10 - 12]). Indeed, the statistical fluctuations of combustion are well handled by the trained ANN-based ionsense sensor which was demonstrated in experiments described by the above mentioned research group [11, 12]. Clearly, a very comprehensive ANN training covering a broad range of possible engine operating conditions would assure the correct data interpretation, at least, in the statistical sense, enough to enhance the performance of the engine control system.

The implementation of an ANN block into the lonsense signal processing defines the sensor electronics. It becomes Digital Signal Processing (DSP)-based with all the issues associated with this technique. The option of designing and manufacturing a dedicated ANN chip seems to be unacceptable due to the cost and lack of algorithm flexibility. The only option seems to be an ANN algorithm, developed as a result of bench training, executed by an on-board microprocessor in real-time. Therefore, the next step in the introduction of lonsense advanced features for mass production would be to prove its ability to operate in real-time with the support of currently available or next generation, automotive-approved, microprocessors. In other words, the assessment of required computation power with a realistically defined signal-processing algorithm becomes a priority in the development activity leading to an advanced version of the lonsense soft sensor. This paper presents an attempt in this direction.

In addition, the troublesome problem of the ANN algorithm formulation that requires extensive, “never guaranteed to be fully complete”, training is addressed. Namely, the proposed approach delivers signal processing results that seem to be immune to some engine combustion fluctuations not included in the ANN training. Although the activity described here is still far from complete, the results presented continue the earlier efforts [11, 12] in implementing statistical methods for lonsense signal processing.

ALTERNATIVE DSP ALGORITHMS

As previously stated, the ANN subsystem requires extensive training on pre-production data samples. Yet, once established, it may represent a simple computational algorithm easily executed either by a dedicated DSP chip or by the on-board microprocessor. The ANN algorithm complexity depends on the input vector size to the first, hidden neuron layer. This complexity directly affects its ability to execute in real-time – between adjacent combustion events. If the Location of Peak Pressure (LPP) is to be extracted from the lonsense signal, the input vector size reflects the eventual system resolution. Specifically, if the required resolution is ½ degree of crank angle, and the window of interest covers, say, 60 degrees, the signal input vector size would be 120. In addition, as previously demonstrated by others [11, 12], the desired correlation between the ANN output and the actual location of peak pressure is acquired only if Manifold Absolute Pressure (MAP), engine speed (RPM), and spark advance (SA) are also fed to the ANN input. This increases the vector size to 123. This is far too large if multi-layer perceptron architecture is to be emulated in real-time. This real-time operation requires a data acquisition period (window) and, beginning with the closure of this window, processing completion prior to the next cylinder event. One of the options available [11] is the input data reduction achieved with the statistical method called Principal Component Analysis (PCA). Briefly, this method [13] generates a new set of input vector

components from a linear combination of the original vector components. All the new components are orthogonal to each other so there is no redundant information. However, it is commonplace for the sum of the variances of the first few new components to almost match the total variance of the components of the original vector. Thus, the new vector can be substantially downsized without a significant loss in the information needed for further processing. In the language of DSP, it means that the algorithm is introduced, in the form of a matrix consisting of 120 input elements (the initial vector size of the lonsense signal in our example) and, say, an output consisting of 10 elements. Such a size reduction was proven not to affect the outcome of the ANN processing when used for lonsense data interpretation [11]. Input data reduction from 123 elements to 13 elements (reduced in size to a 10 element lonsense vector plus MAP, RPM, and SA) makes even a fairly complex ANN emulation feasible in real-time at all engine speeds. The application of the PCA, however, does not come without penalty. Following our example, the PCA method translates to an additional algorithm represented by a matrix consisting of 120 rows (input size), and 10 columns (output size). The reduced output is a result of matrix multiplication performed on the 120-element lonsense vector input. This matrix multiplication actually consumes more computer power than any ANN algorithm used in our experiments. As is shown below, this defines a limit for the maximum engine speed within which our experimental set-up (modeled in Mathworks’ Simulink) could operate in real-time, given available signal processing speed and resources. To illustrate DSP resource requirements for a typical ANN-based ion current soft sensor supported by a PCA data reduction matrix, an estimate was made for an algorithm emulating a 15-neuron hidden layer and 1-neuron output layer. It was assumed that the hidden layer is fed from a PCA matrix having 10 outputs plus three key engine operating parameter (MAP, rpm, Spark Advance) for a total of 13 elements. The results are presented in Table 1. In the process of calculating number of multiply-accumulate instructions it was found that more than 2/3 must be allocated to serve the PCA data reduction matrix!

	Motorola 683XX	Motorola DSP 56800	Motorola PowerPC500
Clock Speed	32 MHz	150 MHz	50 MHz
Execution Time	5.3 ms	50 μs	110 μs
A/D Conversion	14 μs	6 μs	8 μs

Table 1. An example of DSP Resource Requirements for a Typical Ion Current Soft Sensor (a PCA data reduction matrix providing 13 inputs to the ANN consisting of 15-neuron hidden layer and 1-neuron output layer). Resource requirements are calculated for a sampling rate of 40 kHz.

The application of the Principal Component Analysis defines the risk, or better, the robustness of the lonsense soft sensor. As long as the PCA is formulated with extensive pre-production collected data sets and the ANN is subsequently well trained, the system guarantees valued performance. That is due to the fact that once the algorithm is formulated, it can be executed in real-time with a known, pre-defined statistical error. However, the statistical error is guaranteed to remain within the limit established in pre-production tests only if all real-time conditions are covered during the PCA formulation and ANN training phase. This is partly due to the fact that the ANN represents artificial intelligence; it cannot perform any better, or extrapolate beyond, what it was taught during training. Another limitation results from the input signal transformation performed by the PCA matrix. An orthogonal set of components of the linearly transformed ion current signal remains nearly orthogonal as long as any in-service, real-time input closely emulates past signals used in the pre-production training. However, if the in-service signal characteristics differ substantially from those the system was exposed to during PCA matrix formulation, the PCA output compromises the transformation, the output becomes strongly non-orthogonal, and the whole system fails. Consequently, the lonsense soft sensor supported by the PCA/ANN algorithm guarantees faultless operation only if the pre-production algorithm formulation, including the ANN training, resulted from an experimental data set representing all future engine operating conditions. In practice, this might be impossible or at least extremely time and resource consuming. The only reasonable solution, in the case discussed here, seems to be a limited training with well chosen, most-representative sets of operating conditions. Then, possibly together with a fuzzy logic block overruling unusual sensor readings, the lonsense system would enhance the engine controller performance under "typical" driving conditions.

The system robustness could be substantially improved if the ANN training is conducted with inputs representing straightforward factors defining engine thermodynamics rather than their coded version in the form of the lonsense signal. An example of such an approach would be to feed to the ANN the position of a local, post-flame lonsense peak, which theoretically represents the culmination of the compression-induced heating [1]. Now, the input deals with a component having a clear meaning rather than a fuzzy-defined, stochastic representation of the combustion process, i.e., the whole lonsense signal. Then, not only is the size of the input to the ANN substantially reduced, but also, since the post-flame, local lonsense peak correlates well with the location of peak pressure, the system could serve as a virtual in-cylinder pressure sensor. Reported [1] correlation between lonsense post-flame local peak location and true location of peak pressure is close to 80% and can be substantially improved if the ANN is trained with side parameters such as spark advance, engine speed, and engine load.

Attempts to recover information on the post-flame local lonsense peak have been reported by others [14]. Unfortunately, the proposed parameterization of the lonsense signal by curve fitting (employing Gaussian functions) may fail if the local lonsense peak in question is not well pronounced. It may also require intensive computations that may be beyond what current generation microprocessor can handle in real-time.

If the same technique is used to recover air-to-fuel ratio information encoded in the flame front, ion current peak location provides even less impressive results. Not only the peak location, but also its magnitude and integral over the flame front zone are needed. The species ionization in the combustion zone, however, is without any doubt represented by the lonsense signal (see for example Langmuir probe characteristics and discussion of their interpretation in [15] or [16]). Therefore, the key to extracting the encoded information seems to be efficient filtration and processing to unmask and identify certain desired signal features. Since the signal features in question are not solely characterized by the frequency spectrum, their position on the time or angular scale is critical. Wavelet-based signal processing seems to provide the right tool. A side benefit of such a technique is the fact that the wavelet filter is a digital filter with a low level of complexity. Therefore, it makes an ideal, computationally-efficient algorithm representation in the DSP system.

Our bench test results for both data reduction methods supporting the ANN data interpretation block are depicted in Figures 1A and 1B. One algorithm emulated the PCA/ANN approach while the other used Wavelet-based extraction of three signal features considered critical for efficient neural network training. Consequently, the size of the input vector to the ANN preceded with the PCA matrix was 10 elements along with key engine operating parameters, while the input vector size to the ANN preceded with the Wavelet filter was only 3 elements plus the same engine parameters. Considering the fact that the ANN training results are slightly different each time the training is performed, even with the same set of the input data, the soft sensor seems to deliver the same performance regardless of the data reduction method.

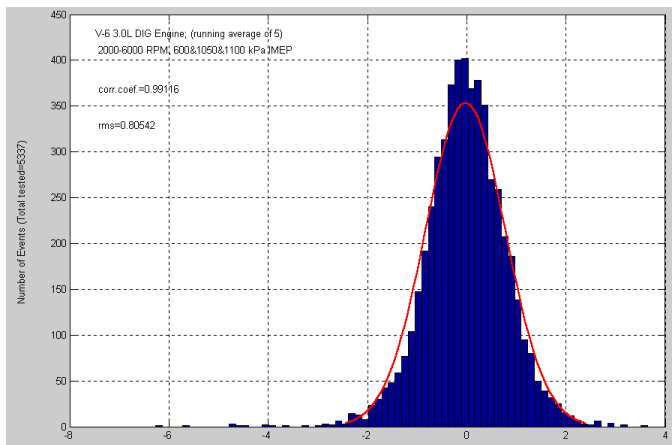


Figure 1A: Soft ionsense, ANN-based sensor performance in detecting location of peak pressure position using the PCA matrix input data reduction. Correlation coefficient = 0.99146, RMS = 0.80542

improved angular resolution, especially at low engine speeds.

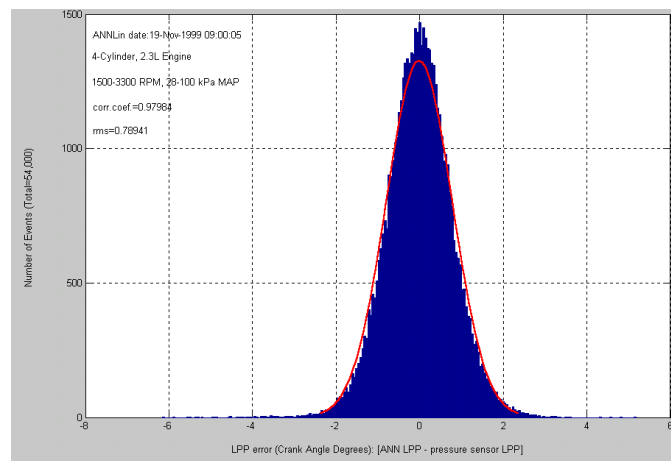


Figure 2: ionsense LPP performance for a different engine from that represented in Figure 1 and slightly compromised sampling rate. Correlation coefficient = 0.97984, RMS = 0.78941

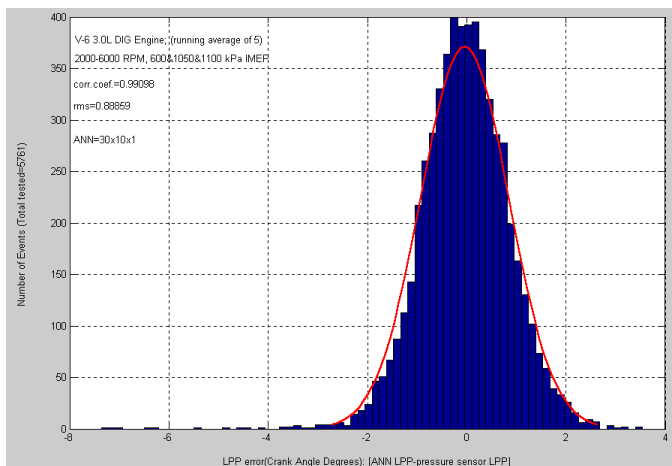


Figure 1B: Soft ionsense, ANN-based sensor performance in detecting location of peak pressure position using the Wavelet-based signal feature extraction. Correlation coefficient = 0.99098, RMS = 0.88859

While the LPP feature is clearly correlated with the local, post-flame ion current peak location, other advanced diagnostics may be strongly affected by the fuel type and fuel contaminants. Both affect the ionsense signal (illustrated in Figure 3A).

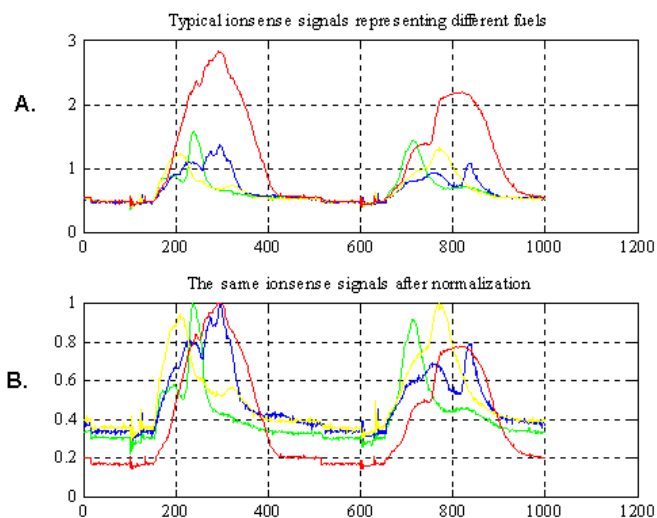


Figure 3: An example of ionsense signals acquired when different fuel types and different fuel contaminants were used. A – original ionsense signals B – same signals normalized. Fuels used: Standard 87 octane, Standard 87 octane+10% ethanol, California Phase II, Standard 87 octane + 10% ethanol + commercial fuel additive.

The performance of the soft ionsense LPP sensor depends on the engine type since the ion current represents a “signature” of the engine’s unique thermodynamics. Consequently, the ANN architecture would vary with engine type, and would require application-specific training. Nevertheless, the ultimate sensor performance is similar regardless of the engine type (see Figure 2) and, in the case of LPP, depends on the sampling rate to define the resolution of the system. The results presented in Figure 2 are based on an engine speed-adjustable sampling rate to maintain a constant resolution of 1 crank angle degree per sample. Slightly better results (see Figure 1) are achieved with a constant sampling rate of 40 kHz, which provides

While the content of different crude oil fractions, ethanol, etc., certainly affect combustion thermodynamics, other additives, offered to “increase engine performance”, may strongly affect the electrical conductivity of the flame [15, 16] and thus alter the Ionsense signal amplitude. Typical examples of the latter are commercial fuel additives containing alkalis that dramatically boost flame conductivity. Therefore, when the air-to-fuel ratio is to be extracted from the Ionsense signal, input signal normalization may be needed to compensate for combustion thermodynamic irrelevant effects. An example of such normalization is depicted in Figure 3 B. Since the normalization might be performed against any specific feature of the Ionsense signal, improved results are obtained if the signal processing is tuned to extract such a feature. This again indicates that the Wavelet-based algorithm formulation may be superior to the PCA approach.

An example of Air/Fuel Ratio (AFR) soft sensor performance with data acquired over a broad range of engine operating conditions, with four different fuel compositions, is depicted in Figure 4.

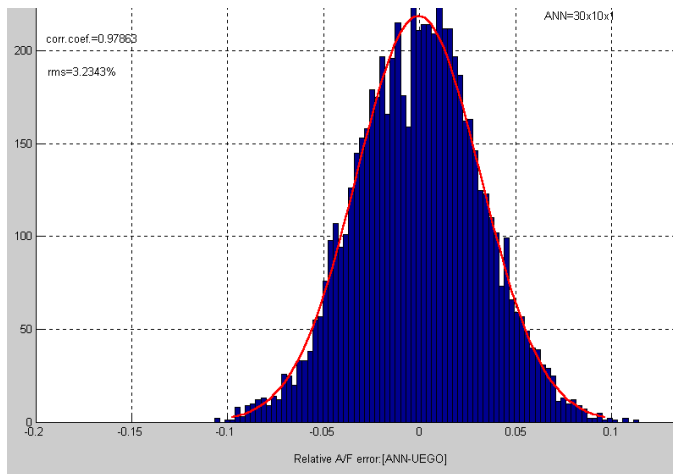


Figure 4: Ionsense Relative Air Fuel Ratio (λ) performance for an experiment run with four different fuel compositions: Standard 87 octane, Standard 87 octane + 10% ethanol, California Phase II, Standard 87 octane + ethanol + commercial fuel additive. Correlation coefficient = 0.97863, RMS = 3.2343%

It must be stated that the cycle-to-cycle, stochastic, fluctuation of Ionsense signal strongly affects sensor performance. The above results (for both LPP and λ) represent running averages of 5 consecutive individual cylinder combustion events. Figure 5 indicates how the number of events averaged influences the sensor output accuracy. In this data, the ripples appearing for averages created over 50 consecutive events are due to the data acquisition routine rather than any real system performance. It is evident that the running average of 3 to 10 most likely defines the best compromise between system accuracy and response time.

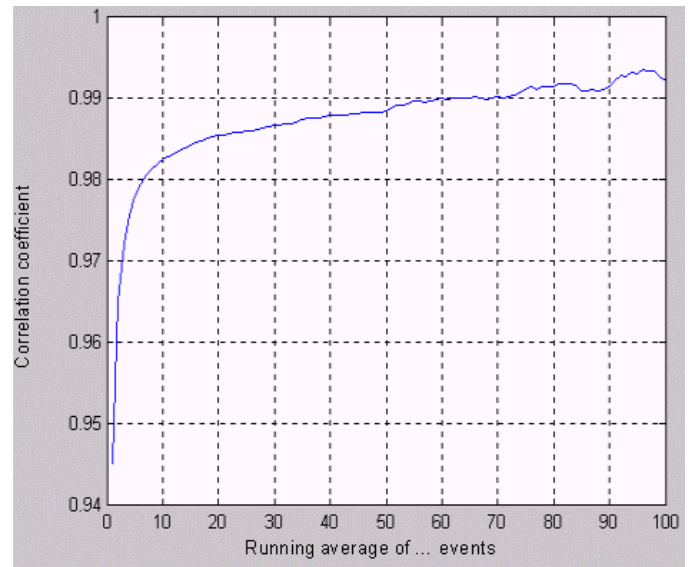


Figure 5A: Soft-sensor response as a function of number of consecutive combustion events taken as a running average – Statistical Correlation

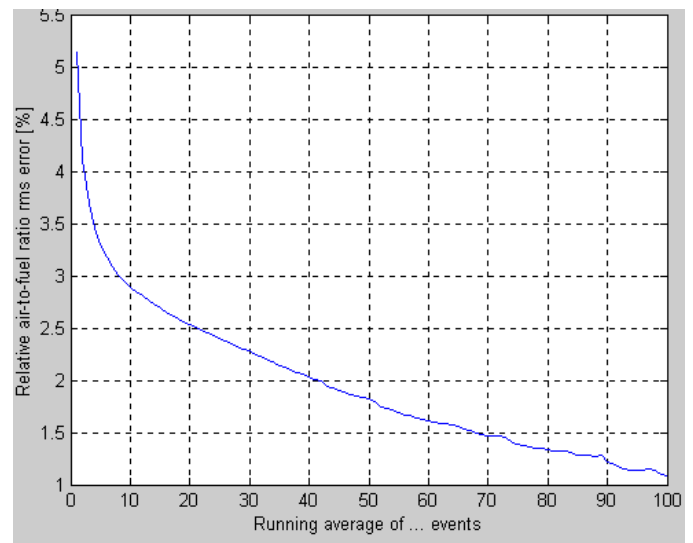


Figure 5B: Soft-sensor response as a function of number of consecutive combustion events taken as a running average – RMS Error.

While the air-to-fuel ratio performance presented here clearly indicates that the Ionsense method cannot replace the widely accepted Narrow-Band (stoichiometric switching) Oxygen Sensor, it may compete favorably with the Wide-Band Oxygen Sensors used in some applications. A niche for this application may also exist for monitoring the Air/Fuel Ratio during cold starts or possibly with advanced On-Board Diagnostics.

EXPERIMENTAL SETUP AND REAL-TIME EXPERIMENT

Due to the sensitivity of the proposed algorithms to the sampling rate of the analog lonsense signal, the data acquisition system targeting a bench-type neural network training sequence was combined with a real-time functional model. Such an arrangement assures that the data reduction and ANN blocks will be exposed to identically phased signals when training and when serving as a real-time soft sensor. A block diagram of the lonsense Location of Peak Pressure soft-sensor utilizing the PCA data reduction matrix is presented in Figure 6. The pre-production data acquisition stage requires storage of the lonsense signal array, together with engine speed, MAP, and spark advance. In addition, the Location of the Peak Pressure extracted from the independent in-cylinder pressure sensor is stored and used for ANN training. Once the PCA matrix is defined and the ANN trained, the full algorithm emulated by the block diagram is engaged. This allows verification in real-time of the PCA/ANN system performance. A mass produced version would, of course, not employ an in-cylinder pressure transducer.

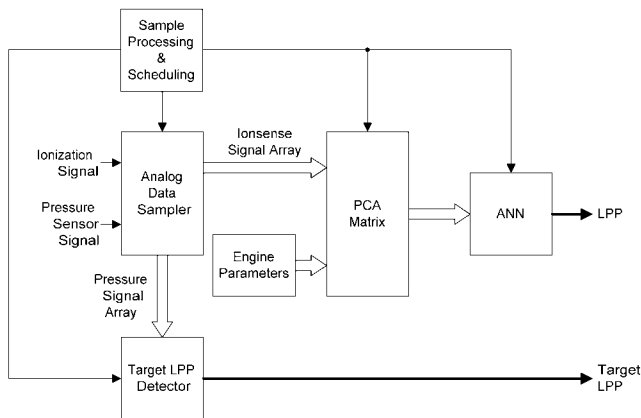


Figure 6: Simplified functional block diagram representing LPP extraction algorithm utilizing the PCA matrix for data reduction.

As presented in Figure 7, the λ extractor utilizes a wavelet filter bank instead of the PCA matrix. The software “architecture” becomes dramatically simplified. The code processes a sequential flow of consecutive data points arriving from the A/D converter instead of the lonsense vector array required by the PCA approach. The input of the ANN block receives essential information for data interpretation in the form of signal features representing “physics of the process” rather than statistical information that may be incomplete if the PCA matrix design is compromised, say, due to experimental limitations.

A side benefit of using the Wavelet approach is the availability of the compressed lonsense signal data. For example, if a three-level decomposition block is used (a fair assumption for most lonsense applications), the achieved compression is 1/8th the original data size. This might be critical in pre-production testing when a very extensive data set must be collected for successful ANN training. The PCA version would obviously require 8-times more data storage.

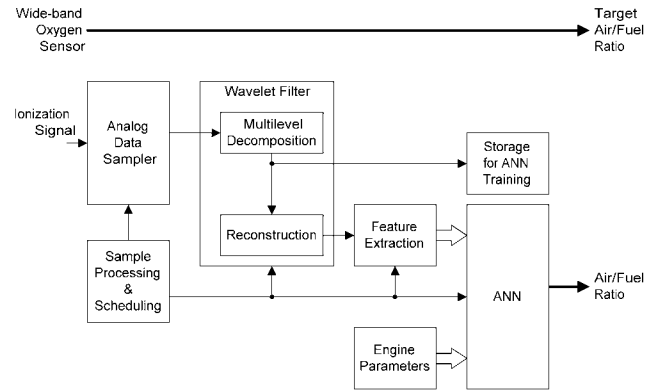


Figure 7: Simplified functional block diagram utilizing a wavelet filter bank for data extraction.

The depicted system extracts AFR information from the lonsense signal. Now, instead of formulating the PCA matrix preceding the ANN training as in the PCA/ANN approach, the ANN can be trained as depicted in Figure 8.

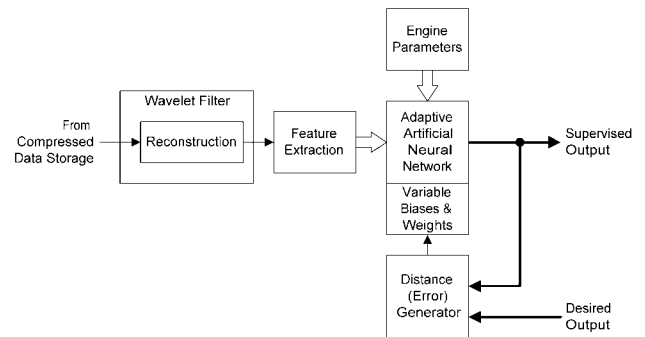


Figure 8: The ANN training with data acquired with a multi-level wavelet decomposition filter.

The ANN training should cover inputs representing a wide range of engine operating conditions. Training is performed via the playback of data acquired earlier; such data acquisition may include dynamometer and road tests. Once the supervised output meets a desired quality standard, the computational algorithm can be frozen. It will then become a part of the global control algorithm for the specific type of engine.

Both, PCA/ANN and Wavelet/ANN algorithms were emulated using Mathworks' Simulink, DSP Blockset, and Neural Network toolboxes [17]. The capability of performing the required computations in real-time was demonstrated using Mathworks' Real-Time Interface and dSPACE (GmbH) PC-based hardware. A 480 MHz, Motorola Power PC-based DS1005 board together with appropriate A/D conversion and timing boards was used. The following configurations were real-time tested:

1. **AFR model supported by a wavelet filter bank:**
The model was operated with a constant sampling rate of 40 kHz and with synchronization of the Sampling Window & Data Trigger Block (see Figure 7) provided by Electronic Spark Timing (EST) pulses.
2. **LPP model supported by a PCA matrix:**
When EST pulses were used to synchronize the Sampling Window & Data Trigger block, the sampling rate was limited to 35 kHz. The slower sampling rate is due to the fact that PCA data reduction matrix is more complex than the wavelet filter and the DS1005 board cannot support higher sampling rates in real-time. In other system embodiments, however, a DS4002 timing board was implemented to replace the functionality of the Sample Window & Data Trigger block. It is also synchronized with EST pulses, yet liberates enough computation power to allow for faster sampling rates. In this arrangement, the system operates as an asynchronous model in the sense that data acquisition block trigger rate varies while the software timebase is a constant 50 kHz. A variable sampling rate, in turn, allows maintaining a near constant distance between samples on the crankshaft angular scale regardless of the engine speed.

An instrument panel emulated when running a real-time experiment with the Control Desk software offered by dSPACE is illustrated in Figure 9.

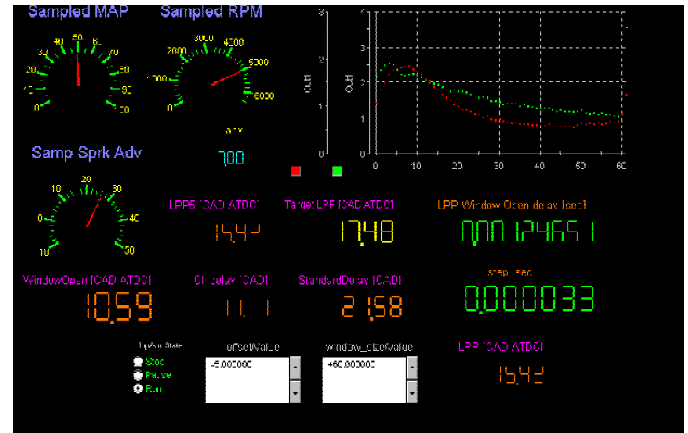


Figure 9: dSPACE dashboard emulation when running LPP soft sensor in real-time.

The throughput demand was assessed for individual subsystems. It was found that the critical demand is made during pre-processing (windowing, data sampling, and feature extraction/data reduction) rather than post-processing (ANN). With one sample per Crank Angle Degree, the maximum required sample rate is 36 kHz at 6000 rpm. With the asynchronous model, the sampling rate could be increased up to 180 kHz with no observed throughput problems. It is believed that post-processing occurs sufficiently fast enough to not be a problem at high speed even in eight-cylinder applications.

The AFR feature, however, suffers from another limitation when lonsense technology is combined with the inductive ignition system. The early opening of the sampling window (required to extract flame-front zone features) experiences strong interference from the coil ringing. Typically, coil ringing masks the majority of the AFR information in the signal at engine speeds above 3000 rpm.

CONCLUSION

The capability of performing the required computations in real-time was demonstrated using both the PCA/ANN and Wavelet/ANN models with a relatively high degree of architecture complexity. The low-pass decomposition segment of a wavelet filter bank allows for significant reduction of ionization current data storage, which may be critically important when collecting an extensive database for ANN training. At the same time, the feature extraction inherently associated with wavelet transformation (pattern recognition) facilitates the soft lonsense engine diagnostic application. Intuitively, the extraction of lonsense signal features supported by the thermodynamics and chemistry of combustion should provide results more immune to situations not covered during the ANN training. In addition, the wavelet-based signal filtering and data reduction method proves to be more throughput-efficient. Conversely, the ANN trained with data-reduced parameters provided by the statistical PCA matrix requires more DSP resources and is certainly not immune to input variation not covered by the pre-production matrix formulation. The next generation of on-board automotive microprocessors will certainly facilitate the implementation of advanced lonsense features for engine diagnostic and control applications.

ACKNOWLEDGMENTS

The authors wish to express their appreciation for the assistance of Messrs. S. Jogi and D. Saldano, both with Technical Support of dSPACE, Novi, MI, and Mr. M. Temple of Delphi's Technical Center, Brighton, MI for invaluable support in preparing and running real-time experiments.

REFERENCES

1. A. Saitzkoff, R. Reinmann, F. Mauss, M. Glavmo, "In-Cylinder Pressure Measurements Using the Spark Plug as an Ionization Sensor," SAE paper No. 970857, 1997.
2. R. Reinmann, A. Saitzkoff, F. Mauss, "Local Air-Fuel Ratio Measurements Using the Spark Plug as an Ionization Sensor," SAE paper No. 970856, 1997.
3. C. Bowman, "Kinetics of Pollutant Formation and Destruction in Combustion," Prog. Energy Combust. Sci., Vol. 1, pp 33-45, 1975.
4. C. Daniels, "The Comparison of Mass Fraction Burned Obtained from the Cylinder Pressure Signal and Spark Plug Ion Signal," SAE paper No. 980140, 1998.
5. M. Kramer, K. Wolf, "Approaches to Gasoline Engine Control Involving the Use of Ion Current Sensory Analysis," SAE paper No. 905007, 1990.
6. J. Forster, A. Gunther, M. Ketterer, K. -J. Wald, "Ion Current Sensing for Spark Ignition Engines," SAE paper No. 1999-01-0204.
7. D. Upadhyay, G. Rizzoni, "AFR Control on a Single Cylinder Engine using the Ionization Current," SAE paper No. 980203, 1998.
8. R. Reinmann, A. Saitzkoff, B. Lassesson, P. Strandh, "Fuel and Additive Influence on the Ion Current," SAE paper No. 980161, 1998.
9. J. Keck, J.B. Heywood, G. Noske, "Early Flame Development and Burning Rates in Spark Ignition Engines and Their Cyclic Variability," SAE paper No. 870164, 1987.
10. N. Wickstrom, M. Taveniku, A. Linde, M. Larsson, B. Svensson, "Estimating Peak Pressure Position and Air-Fuel Ratio Using the Ionization Current and Artificial Neural Networks," Proceedings of IEEE Conference on Intelligent Transportation Systems, Boston, November 9-12, 1997
11. M. Hellring, T. Munther, T. Rongvaldsson, N. Wickstrom, C. Carlsson, M. Larsson, "Spark Advance Control using the Ion Current and Neural Soft Sensors," SAE 1999-01-1162
12. M. Hellring, T. Munther, T. Rongvaldsson, N. Wickstrom, C. Carlsson, M. Larsson, Jan Nytomt, "Robust AFR Estimation Using the Ion Current and Neural Networks," SAE 1999-01-1161.
13. I.T. Jolliffe, "Principal Component Analysis," Springer-Verlag New York Inc., 1986.
14. H. Klovmark, P. Rask, U. Forssell, "Estimating the Air/Fuel Ratio from Gaussian Parametrizations of the Ionization Currents in Internal Combustion SI Engines," SAE Paper No. 2000-01-1245.
15. A. G. Gaydon, H. G. Wolfhard, "Flames; Their structure, radiation and temperature," Chapman and Hall Ltd., 1970.
16. J. Lawton, F. J. Weinberg, "Electrical Aspects of Combustion," Clarendon Press, Oxford 1969.
17. See the relevant User's Guides published by The MathWorks Inc.